Electron-impact ionization of moderately charged atomic ions in excited states

M. S. Pindzola, C. P. Ballance, and S. D. Loch
Department of Physics, Auburn University, Auburn, Alabama, USA
(Received 11 March 2011; published 15 June 2011)

Nonperturbative *R*-matrix and perturbative distorted-wave methods are used to calculate electron-impact ionization cross sections for C^{3+} in excited states. Convergence studies for the cross sections of the $1s^25s$ excited configuration reveal that both the *R*-matrix and distorted-wave methods need fairly high ejected electron angular momenta. Reasonable agreement is found between the converged *R*-matrix and distorted-wave cross sections. Thus, the use of the computationally less demanding distorted-wave method as a tool for the n scaling of excited-state ionization cross sections appears to be reasonable for atomic ions with charge $q \geqslant 3$.

DOI: 10.1103/PhysRevA.83.062705 PACS number(s): 34.80.Dp, 34.50.Fa

I. INTRODUCTION

Accurate electron-impact ionization cross sections involving the excited states of atomic ions are needed for the collisional-radiative modeling of the moderately dense plasmas found in magnetic fusion energy experiments [1,2]. For neutral atoms and low-charged atomic ions, nonperturbative close-coupling methods have been found to give more accurate excited-state ionization cross sections than perturbative distorted-wave methods. *R*-matrix with pseudostates calculations have been carried out for excited states of H up to $4l$ [3], Li^{2+} up to $4l$ [3], B up to $1s^22s^24l$ [4], B^+ up to $1s^22s4l$ [4], and B^{2+} up to $1s^25l$ [4]. Convergent close-coupling calculations have also been carried out for excited states of He up to $1s4l$ [5] and He^+ up to $4l$ [6].

Since the nonperturbative close-coupling methods are generally very computationally intensive, it would be of interest to know at what charge state of an atomic ion one could expect to obtain accurate excited-state ionization cross sections using perturbative distorted-wave methods. While this has been investigated for ground-state ionization, it is an open question for excited-state ionization. Lee *et al.* [4] showed that one could use nonperturbative cross section results to evaluate a scaling parameter to be applied to semiempirical expressions for B, B^+, and B^{2+}. These scaled semiempirical results could then be easily used to produce accurate ionization cross sections for higher n shells. Thus, as well as investigating when distorted-wave results become accurate for excited-state ionization, we also seek to find a scaling parameter that can be used with a semiempirical expression to obtain accurate results for the higher n shells of C^{3+}.

In this paper, we examine electron-impact ionization cross sections for the $1s^25s$ excited configuration of C^{3+}. Large-scale nonperturbative *R*-matrix with pseudostates calculations are carried out to determine the accuracy of perturbative distorted-wave calculations. Previous nonperturbative convergent close-coupling [7], time-dependent close-coupling [8], and *R*-matrix with pseudostates [8,9] calculations were found to give cross sections for ionization of the $1s^22s$ ground configuration of C^{3+} that were slightly above and below results from perturbative distorted-wave calculations [8].

The rest of the paper is organized as follows: In Sec. II we give a brief review of the *R*-matrix with pseudostates and configuration-average distorted-wave methods as applied to electron-impact single-ionization processes, in Sec. III we present results for the electron-impact ionization of excited states of C^{3+}, and in Sec. IV we present our conclusions. Unless otherwise stated, all quantities are given in atomic units.

II. THEORY

A. *R*-matrix with pseudostates (RMPS) method

The *R*-matrix method was first applied to calculate cross sections for the electron-impact excitation of atoms and their ions [10]. The method was extended to calculate cross sections for the electron-impact ionization of atoms through the introduction of large numbers of pseudostates [11,12].

Inside the *R*-matrix box, the total wave function for a given LS symmetry is expanded in basis states given by

$$\Psi_k^{N+1} = A \sum_{i,j} a_{ijk} \psi_i^{N+1} \frac{u_j(r_{N+1})}{r_{N+1}} + \sum_i b_{ik} \chi_i^{N+1}, \quad (1)$$

where A is an antisymmetrization operator, ψ_i^{N+1} are channel functions obtained by coupling N-electron target states with the angular and spin functions of the scattered electron, $u_j(r)$ are radial continuum basis functions, and χ_i^{N+1} are bound functions which ensure completeness of the total wave function. The coefficients a_{ijk} and b_{ik} are determined by diagonalization of the total $(N+1)$-electron Hamiltonian. On massively parallel computers the diagonalization for all eigenvalues and eigenstates is made over many processors using a numerical subroutine from the SCALAPACK library [8].

Outside the *R*-matrix box, the total wave function for a given LS symmetry is expanded in basis states given by

$$\Psi_k^{N+1} = \sum_i \psi_i^{N+1} \frac{v_i(r_{N+1})}{r_{N+1}}. \quad (2)$$

The radial continuum functions, $v_i(r)$, are solutions to the coupled differential equations given by

$$T_i(r)v_i(r) + V_{ij}(r)v_j(r) = 0, \quad (3)$$

where $T_i(r)$ is a kinetic and nuclear energy operator and $V_{ij}(r)$ is an asymptotic coupling operator. Above the ionization threshold the coupled differential equations may be solved on a coarse energy mesh. On massively parallel computers a simple parallelization, with no message passing, is made over the incident electron energies [13]. The inner and outer solutions are matched at the edge of the *R*-matrix box and the

K matrix is extracted. Excitation and ionization cross sections are determined by relating the K matrix to the S matrix. The target radial orbitals are calculated using the atomic structure code called AUTOSTRUCTURE [14]. The spectroscopic orbitals are determined using a Thomas-Fermi-Amaldi approximation, while the remaining Laguerre pseudo-orbitals are orthogonalized to the spectroscopic orbitals and to each other.

B. Configuration-average distorted-wave (CADW) method

The configuration-average distorted-wave (CADW) expression for the electron-impact single-ionization cross section of the $(n_t l_t)^{w_t}$ subshell of any atom is given by [15]

$$\sigma_{\rm single} = \frac{16 w_t}{k_i^3} \int_0^E \frac{d\epsilon_e}{k_e k_f} \sum_{l_i,l_e,l_f} (2l_i+1)(2l_e+1)(2l_f+1) \times \mathcal{P}(n_t l_t, k_i l_i, k_e l_e, k_f l_f), \quad (4)$$

where the linear momenta (k_i,k_e,k_f) and the angular momenta (l_i,l_e,l_f) quantum numbers correspond to the incoming, ejected, and outgoing electrons, respectively. The total energy $E = \epsilon_i - I = \epsilon_e + \epsilon_f$, where I is the subshell ionization energy and $\epsilon = \frac{k^2}{2}$. The first-order perturbation theory expression for the scattering probability $\mathcal{P}(n_t l_t, k_i l_i, k_e l_e, k_f l_f)$ is given in terms of standard $3j$ and $6j$ symbols and radial Slater integrals [15].

The bound radial orbitals, $P_{nl}(r)$, needed to evaluate the Slater integrals are calculated using a Hartree-Fock atomic structure code [16]. The continuum radial orbitals, $P_{kl}(r)$, needed to evaluate the Slater integrals are calculated by solving the radial Schrödinger equation using a Hartree with local exchange potential. For N bound target electrons, the incident and scattered electron continuum radial orbitals are evaluated in a V^N potential, while the ejected continuum radial orbital is calculated in a V^{N-1} potential [17]. Alternatively, the incident, ejected, and scattered electrons are all calculated in a V^{N-1} potential [18]. The continuum normalization for all the distorted waves is one times a sine function.

III. RESULTS

We first carried out RMPS calculations for the electron-impact ionization of the C^{3+} $1s^2 5s$ excited configuration. The target radial wave functions for C^{3+} were generated using a Java front end for the atomic structure code AUTOSTRUCTURE [14]. A continuum basis of 35 was used to span the incident electron energy range between 0 and 50 eV, which given the high n shell nature of this study is easily enough to delineate the peak of the ionization cross section. An exchange calculation was carried out for incident partial waves l_i ranging from 0 to 35, with a top-up procedure implemented to account for the contribution from the higher incident partial waves. An energy mesh of 0.01 Ry was used in the calculation of the total cross section.

Electron-impact ionization cross sections for the $C^{3+}1s^2 5s$ excited configuration calculated using the RMPS method are presented in Fig. 1. To study the convergence of the total cross section with the angular momentum of the ejected electron, we used various scattering models in which we gradually increased the angular momentum of the pseudo-orbitals. In our first model, the Laguerre pseudo-orbitals ranged in principal quantum number from $n = 6$ to 16 and angular momentum $l_e = 0$ to 6, in our second model the angular momentum ranged from $l_e = 0$ to 8, and in our third and largest model the angular momentum ranged from $l_e = 0$ to 10. The first model has 91 orbitals in the close-coupling expansion, the second model has 108 orbitals and computationally took twice as long, and the third model has 143 orbitals and computationally took five times as long as the first model. The models were chosen to clearly exhibit the convergence issues involved in the high n shell ionization of multiply charged atomic ions. As can be seen in Fig. 1, while there are oscillations in the $5s$ ionization cross section at lower energies due to the difficulty in including enough pseudostates in the near-threshold region, the total cross section appears to have converged by $l_e = 10$ for the ejected electron.

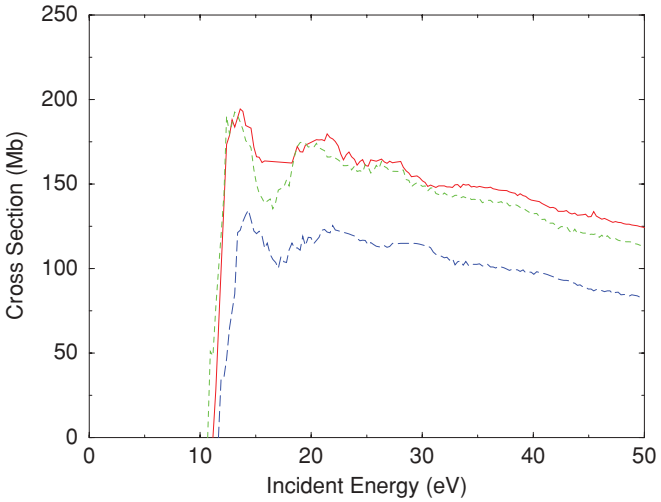

FIG. 1. (Color online) Electron-impact ionization cross sections for the C^{3+} $1s^2 5s$ configuration. Solid (red) curve: RMPS for $l_e = 10$, short dash (green) curve: RMPS for $l_e = 8$, long dash (blue) curve: RMPS for $l_e = 6$ (1 Mb $= 10^{-18}$ cm^2).

Electron-impact ionization cross sections for the $C^{3+}1s^2 5s$ excited configuration calculated using the CADW method are presented in Fig. 2. Hartree-Fock calculations [16] for the C^{3+} $1s^2 5s$ and C^{4+} $1s^2$ configurations yielded a $5s$ ionization potential of 9.3 eV. CADW calculations were made at 5 incident energies ϵ_i, ranging from 1.1 to 5.0 times the ionization potential, and at 25 ejected energies ϵ_e. The continuum radial orbitals were calculated using V_{if}^N and V_e^{N-1} scattering potentials [17]. The number of incident partial waves l_i ranged from 0 to 50 and the number of ejected partial waves l_e was varied between 6 and 14. Since ionization is from an s wave orbital, the number of terms in the multipole expansion for the $\frac{1}{|\vec{r}_1-\vec{r}_2|}$ interaction operator also varies between 6 and 14. As can be seen in Fig. 2, the CADW calculations for the $5s$ ionization cross section are fully converged by $l_e = 14$.

Electron-impact ionization cross sections for the $C^{3+}1s^2 5s$ excited configuration, calculated using both the RMPS and CADW methods, are presented in Fig. 3. The RMPS results for $l_e = 10$ are presented along with a fit to smooth out the pseudoresonances. The CADW results for $l_e = 14$ using V_{if}^N and V_e^{N-1} potentials [17] are found to be slightly larger than the

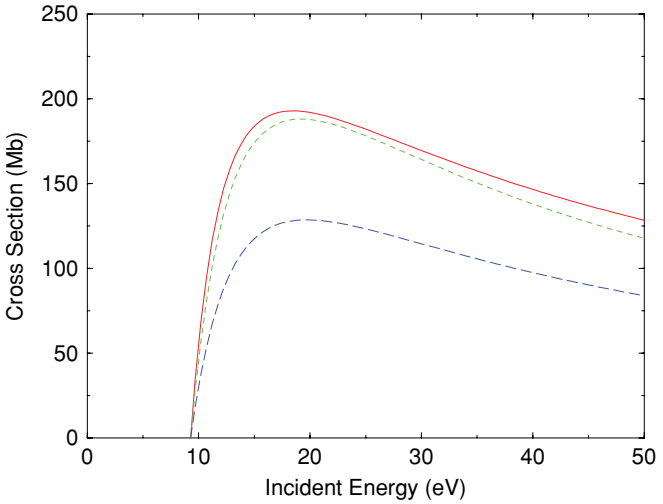

FIG. 2. (Color online) Electron-impact ionization cross sections for the C^{3+} $1s^2 5s$ configuration. Solid (red) curve: CADW for $l_e = 14$, short dash (green) curve: CADW for $l_e = 10$, long dash (blue) curve: CADW for $l_e = 6$ (1 Mb $= 10^{-18}$ cm^2).

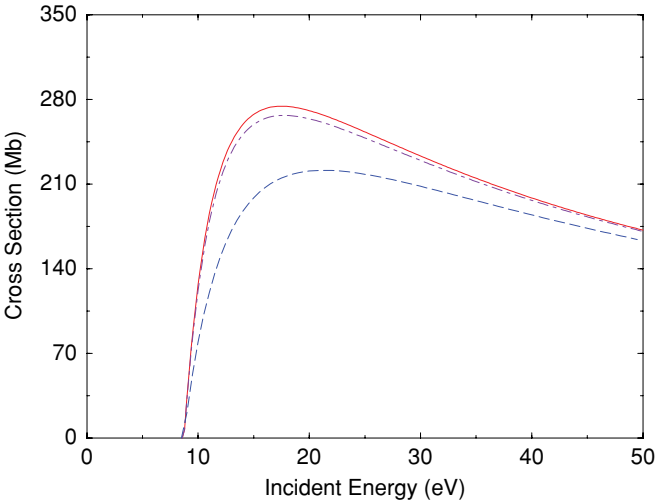

FIG. 4. (Color online) Electron-impact ionization cross sections for the C^{3+} $1s^2 5l$ configurations. Solid (red) curve: CADW with V_{if}^N and V_e^{N-1} bundled over $l = 0$–4, dot-dash (purple) curve: CADW with V_{ief}^{N-1} bundled over $l = 0$–4, long dash (blue) curve: ECIP (1 Mb $= 10^{-18}$ cm^2).

CADW results for $l_e = 14$ using V_{ief}^{N-1} potentials [18]. Overall, the RMPS and CADW ionization cross sections for the C^{3+} $1s^2 5s$ excited configuration are found to be in reasonable agreement.

Electron-impact ionization cross sections for the $C^{3+} 1s^2 5l$ excited configurations calculated using the CADW method are presented in Fig. 4. The bundled l CADW cross sections are obtained by adding individual $\frac{(2l+1)}{25}$ weighted $5l$ cross sections for $l = 0$–4. The CADW results using V_{if}^N and V_e^{N-1} potentials [17] are found to be slightly larger than the CADW results using V_{ief}^{N-1} potentials [18]. We also calculate bundled

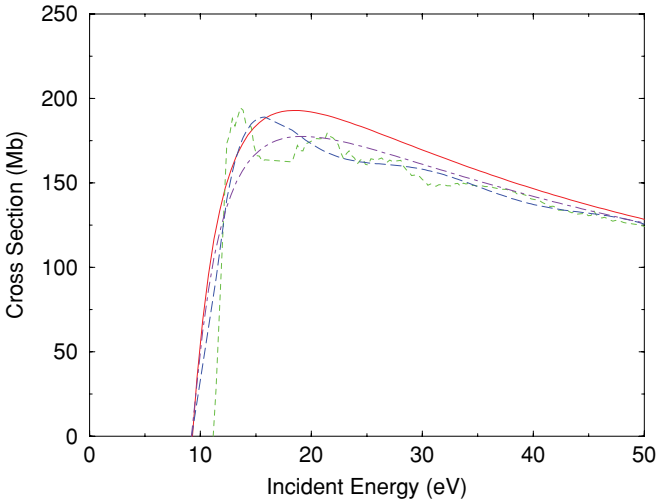

FIG. 3. (Color online) Electron-impact ionization cross sections for the C^{3+} $1s^2 5s$ configuration. Solid (red) curve: CADW with V_{if}^N and V_e^{N-1}, dot-dash (purple) curve: CADW with V_{ief}^{N-1}, short dash (green) curve: RMPS raw, long dash (blue) curve: RMPS fit (1 Mb $= 10^{-18}$ cm^2).

l cross sections using an exchange classical impact parameter (ECIP) expression, due to Burgess and Vriens [19], given by

$$\sigma_{\text{single}} = \frac{4\pi R^2}{E + 2I_n}\left(\frac{5}{3I_n} - \frac{1}{E} - \frac{2I_n}{3E^2}\right), \tag{5}$$

where the ionization potential for the n shell is given by

$$I_n = \frac{R(Q+1)^2}{n^2}; \tag{6}$$

Q is the charge on the atomic ion, E is the energy of the incident electron in eV, and $R = 13.6$ eV. As seen in Fig. 4, the $n = 5$ ECIP cross section for C^{3+} falls below the CADW results. With a scaling factor of approximately 1.2, the ECIP method may be used to extrapolate the $n = 5$ CADW cross section data to higher n shells.

IV. SUMMARY

For neutral atoms and low-charged atomic ions, nonperturbative close-coupling calculations for the electron-impact ionization of ground and excited states have generally found cross sections substantially lower than predicted by perturbative distorted-wave calculations. Correlation effects between the ejected and scattered electrons are strong due to the screening of the nuclear charge and the low collision speeds. The electron-electron interaction is thus not well represented by lowest-order perturbation theory.

In this paper we picked C^{3+} as an example of a moderately charged atomic ion to see whether the nonperturbative RMPS and perturbative CADW methods begin to agree on their prediction of electron-impact ionization cross sections from excited states. In general for atomic ions, the number of ejected angular momenta needed to converge both RMPS and CADW calculations increases for more highly excited states. This is due mainly to the larger radial extent of the excited-state wave function. After a careful check of the

convergence of our RMPS and CADW calculations, we found that the nonperturbative and perturbative cross sections for the electron ionization of the C^{3+} $1s^2 5s$ excited configuration are in reasonable agreement. Perturbative CADW calculations were then carried out for all C^{3+} $1s^2 5l$ ($l = 0$–4) excited configurations. The CADW bundled $5l$ cross sections were then compared to semiempirical ECIP results. Properly scaled ECIP cross sections may now be used to generate all the remaining excited-state ionization cross sections needed for the collisional-radiative modeling of C^{3+} in the moderately dense plasmas found in various astrophysical and laboratory plasmas.

ACKNOWLEDGMENTS

This work was supported in part by grants from the US Department of Energy and the UN International Atomic Energy Agency. Computational work was carried out at the National Energy Research Scientific Computing Center in Oakland, California.

[1] H. P. Summers, W. J. Dickson, M. G. O'Mullane, N. R. Badnell, A. D. Whiteford, D. H. Brooks, J. Lang, S. D. Loch, and D. C. Griffin, Plasma Phys. Controlled Fusion **48**, 263 (2006).
[2] S. D. Loch, C. P. Ballance, M. S. Pindzola, and D. P. Stotler, Plasma Phys. Controlled Fusion **51**, 105006 (2009).
[3] D. C. Griffin, C. P. Ballance, M. S. Pindzola, F. Robicheaux, S. D. Loch, J. A. Ludlow, M. C. Witthoeft, J. Colgan, C. J. Fontes, and D. R. Schultz, J. Phys. B **38**, L199 (2005).
[4] T. G. Lee, S. D. Loch, C. P. Ballance, J. A. Ludlow, and M. S. Pindzola, Phys. Rev. A **82**, 042721 (2010).
[5] Y. Ralchenko, R. K. Janev, T. Kato, D. V. Fursa, I. Bray, and F. J. de Heer, At. Data Nucl. Data Tables **94**, 603 (2008).
[6] I. Bray, I. McCarthy, J. Wigley, and A. T. Stelbovics, J. Phys. B **26**, L831 (1993); [http://atom.curtin.edu.au/CCC-WWW/index.html].
[7] I. Bray, J. Phys. B **28**, L247 (1995).
[8] D. M. Mitnik, M. S. Pindzola, D. C. Griffin, and N. R. Badnell, J. Phys. B **32**, L479 (1999).
[9] M. P. Scott, H. Teng, and P. G. Burke, J. Phys. B **33**, L63 (2000).
[10] P. G. Burke and W. D. Robb, Adv. Atm. Mol. Phys. **11**, 143 (1975).
[11] K. Bartschat, E. T. Hudson, M. P. Scott, P. G. Burke, and V. M. Burke, J. Phys. B **29**, 115 (1996).
[12] T. W. Gorczyca and N. R. Badnell, J. Phys. B **30**, 3897 (1997).
[13] C. P. Ballance and D. C. Griffin, J. Phys. B **37**, 2943 (2004).
[14] N. R. Badnell, J. Phys. B **30**, 1 (1997).
[15] M. S. Pindzola, D. C. Griffin, and C. Bottcher, in *Atomic Processes in Electron Ion and Ion Ion Collisions*, edited by F. Brouillard, NATO ASI Ser. B, 145 (Plenum Press, New York, 1986), p. 75.
[16] R. D. Cowan, *The Theory of Atomic Structure and Spectra* (University of California Press, Berkeley, 1981).
[17] S. M. Younger, Phys. Rev. A **24**, 1278 (1981).
[18] J. Botero and J. H. Macek, J. Phys. B **24**, L405 (1991).
[19] S. M. Younger and T. D. Mark, in *Electron Impact Ionization*, edited by T. D. Mark and G. H. Dunn (Springer-Verlag, Vienna, 1985).